Object-based shell craters classification from LiDAR-derived sky-view factor

Luigi Magnini, Cinzia Bettineschi, Armando De Guio

Angaben zur Veröffentlichung / Publication details:

Magnini, Luigi, Cinzia Bettineschi, and Armando De Guio. 2017. "Object-based shell craters classification from LiDAR-derived sky-view factor." *Archaeological Prospection* 24 (3): 211–23. https://doi.org/10.1002/arp.1565.

Object-based Shell Craters Classification from LiDAR-derived Sky-view Factor

LUIGI MAGNINI*, CINZIA BETTINESCHI AND ARMANDO DE GUIO

Department of Cultural Heritage: Archaeology and History of Art, Cinema and Music, University of Padova, Capitaniato square 7, 35139 Padua, Italy

ABSTRACT This paper presents the results of the first attempt to assess, identify and quantify the residual number of shell craters of World War I currently present in the Vezzena/Luserna/Lavarone Plateau, areas of Millegrobbe, Bisele and Cima Campo (Province of Trento, Italy). Historical sources report the existence of several thousand artillery explosions: therefore, a field survey or a classic photo-interpretation would be labour-intensive and highly time-consuming. For this reason, a digital terrain model (DTM) of the test-site was processed using the Sky-view Factor algorithm and was analysed with an object-based approach, which implied: (1) multiresolution segmentation; (2) classification (main features considered size, shape and colour).
The automatically classified shell craters were thus verified during an *in situ* survey that determined the accuracy of the method in the order of 84% of the total occurrences.

Key words: GeOBIA; LiDAR processing; Sky-view Factor; landscape mapping and monitoring; conflict archaeology; World War I

Introduction

Between 25 May and 28 May 1915, the Italian Forts of Verena and Campolongo attacked the occupants of the Austrian fortification of Cima Campo in one of the most dramatic events of the Great War (World War I) along the fortified line the Vezzena/Luserna/Lavarone plateau (Figure 1).

Numerous historical sources testify to the massive shelling impact in the area. In particular the Memoirs of Augusto Tommasini (1923), officer at the War Tribunal of Trento, speak of 'no less than five thousand projectiles […], especially pieces of 280'.

The plaque on the memorial built in 1918 near the Fort lists the main phases of attack, as well as the type and number of projectiles used. It reads: 'From May the 23th 1915 to May the 20th 1916 the fort underwent 3 major attacks […]. The fort was shot with a total of 200 shells of 30 cm, 8100 of 28 cm and approximately 16000 of 15 cm'.

* Correspondence to: L. Magnini, Department of Cultural Heritage: Archaeology and History of Art, Cinema and Music, University of Padova, Capitaniato square 7, 35139 Padua, Italy. E-mail: luigi.magnini@gmail.com

Now, 100 years later, the material remains of World War I are in various state of post-depositional and post-abandonment processes, involving an increasing loss of information and spatial, physical or functional transformations. Numerous sources of impact – from re-forestation, pedogenesis and relic hunting to building activities – hampered the proper recognition of war-features to such extent that they can be easily confused with different natural or man-made entities. Such an intrinsically fragile archaeological surface is now particularly 'equivocal' and the embedded war scenario must be fully isolated, detected, recognized, enhanced and protected by using the best scientific, intellectual and ethical practices.

In the past two decades the archaeology of World War I has emerged as an attractive and flourishing field, as shown by the abundant specialized literature (for a general overview see Saunders, 2002; Novotny, 2009). Books and papers express a growing interest in material culture (Saunders, 2003, 2012), archaeological excavations and surveys (Fraser and Brown, 2007; Robertshaw and Kenyon, 2008; Desfossés *et al.*, 2009), physical anthropology (Jankauskas *et al.*, 2011; Le Bailly *et al.*, 2012; Gaudio *et al.*, 2013), geophysical prospections (Masters and Stichelbaut, 2009) and

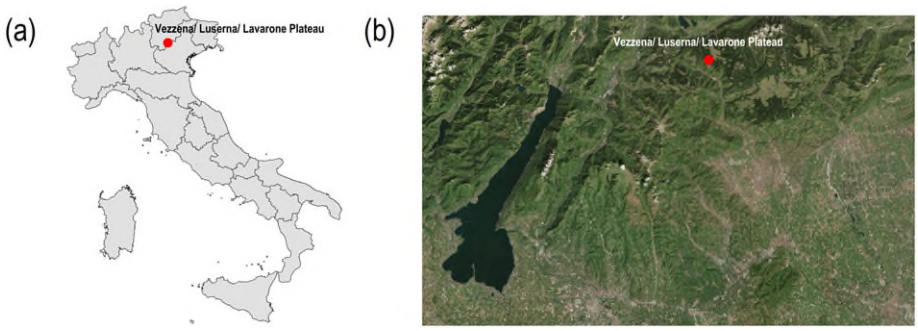

Figure 1. Location of the study area: (a) in the Italian territory with regional boundaries; (b) in the context of northern Italy (Veneto Region). [Colour figure can be viewed at wileyonlinelibrary.com]

remote sensing (Stal *et al.*, 2010; Kaimaris 2011; Hesse, 2014; Gheyle *et al.*, 2016; Mlekuž *et al.*, 2016; Stichelbaut *et al.*, 2016).

In our opinion the last topic, combined with geophysics and ground surveys, seems to offer the best opportunities to detect, protect and monitor the vanishing World War I heritage in the direction of 'minimum tillage' or 'no-collection' policy (aimed at minimizing the archaeological footprint/impact).

Modern landscapes are characterized by a complex evolutionary process whose palimpsestic traces may be very hard to distinguish. Remote sensing techniques possess intrinsic capabilities of object/pattern/scenery recognition and a higher predictive and discriminatory potential that may help to improve the comparability of the analytical data, to reduce the processing time and to avoid errors and bias that can affect the classical archaeological photo-interpretation (Halliday, 2013).

For this purpose, object-based techniques have been increasingly applied to remotely sensed image analysis and classification. The first approaches to object-oriented remote sensing date back to the beginning of the new millennium and to the pioneering work of Blaschke *et al.* (2000). Since 2003 object-based image analysis (also known as OBIA or more properly GeOBIA) spread in forestry sciences, bringing excellent results in mapping tree coverage (Dorren *et al.*, 2003; Heyman *et al.*, 2003). This technique also proved to be a useful tool to solve problems related to the 'salt and pepper' effect typical of the pixel-based classifications (Yu *et al.*, 2006) and to process LiDAR (light detection and ranging) data (Maier *et al.*, 2008).

OBIA has made its way in archaeology only in very limited cases: we could quote the seminal work of Verhagen and Drăgut (2012) on site predictivity through landforms classification or our test studies on semi-automated image analysis of crop and soil marks for sub-surface feature detection (De Guio *et al.*, 2015). A recent paper by Sevara and Pregesbauer (2014) stressed the importance of OBIA experimentation in archaeology with a theoretical approach, while Pregesbauer *et al.* (2014) applied it to the classification of magnetic anomalies. Finally, the methodology has been tested by Sevara *et al.* (2016) in contrast with a pixel-based approach and employed for mound classification in Freeland *et al.* (2016).

Materials and methods

Description of the study area

Millegrobbe, Bisele and Fort Lusern are located in the municipalities of Lavarone and Luserna on a pre-alpine plateau (Province of Trento, Italy) between 1300 and 1600 m above sea level (Figure 2). The natural environment is characterized by lawn terraces that form the focus of a *longue durée* economy of grazing and pasture. The overall emerging phenomenology is a spectacular fossil landscape (Balista *et al.*, 1998), where the cumulative traces of the human activities that contributed to shape the landscape over the

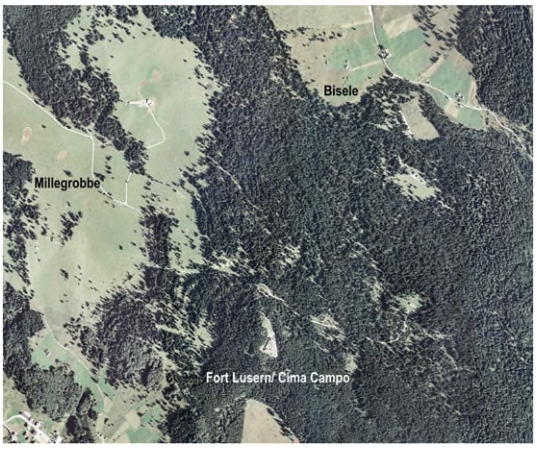

Figure 2. Ortophoto of the study area, located in the municipalities of Lavarone and Luserna (Province of Trento, Italy). [Colour figure can be viewed at wileyonlinelibrary.com]

millennia can still be recognized both at ground level and from aerial (or satellite) view.

The earliest evidences of human occupation date back to the Late and Final Bronze Age (approximately twelfth to the eleventh century BC) and consist of a series of kilns and furnaces connected to the metallurgy of copper. These productive structures are concentrated at the edge of (often still active) mountain pools, which are the only water supply in this karst environment (De Guio, 2005; Addis *et al.*, 2016; Artioli *et al.*, 2016).

In the following centuries, the area was essentially devoted to a mountain economy: woodland exploitation, pastoralism and stone quarries, in a presumptive status of *histoire immobile* (Le Roy Ladurie, 1974), only to return in the forefront of history during World War I.

The construction of Fort Lusern in the area of Cima Campo was a significant source of income for the inhabitants of the plateau in the years before the conflict (1908–1912), as most of the population was (directly or indirectly) involved in the works (Baratter, 2007). Fort Lusern was the most impressive fortification in the area and it was known with the title 'il Padreterno' (the Almighty). Despite its claimed invincibility, the Fort was in serious trouble since the early days of the war, because it occupied a strategic position and was the prime target of Italian artillery shelling.

After three days of non-stop attack the commander Emanuel Nebesar surrendered, fearing the explosion of the fuel depots. The decision was rejected by the other Austrian fortifications and after the symbolic gesture of a volunteer who bothered to remove the white flag, Fort Lusern was re-occupied by the Austrians until the offensive in May 1916 when the front moved (Hentzschel, 2008).

With such different sources of evidence, 'equivocity' or 'equifinality' in feature-formation is a major issue in the recognition and classification of the war scenario [our target warscape, as defined in Korf *et al.* (2010)]. Computer-aided methods of feature extraction seem thus a promising field to tentatively address the problem.

LiDAR data and derived sky-view factor (SVF)

The archaeological application of high-resolution digital elevation models (DEMs) based on airborne LiDAR [sometimes referred to as airborne laser scanning (ALS)] are gaining an increasingly important role for site identification, mapping and monitoring (Hesse, 2010; Zhou and Zhu, 2013).

LiDAR is an active remote sensing technique that enables to calculate the distance from a surface by measuring the time elapsed between the emission of a laser pulse and the reception of the return signal (Weher and Lohr, 1999). The first reflected signals can be filtered to create a DSM (digital surface model) representing the surface of the earth including trees and buildings. However, the last signals are used to build the DTM (digital terrain model), which is a depiction of the bare ground surface under the vegetation canopy (Doneus *et al.*, 2008; Li *et al.*, 2005). Despite the tree cover removal of the DTM, an appropriate data visualization is necessary to identify features of archaeological interest. The most widespread visualization techniques comprise, among others, hillshading, slope gradient, multiple hillshading, PCA (principal component analysis) of hillshading, local relief model, openness, local dominance, cumulative visibility, accessibility, exaggerated relief and SVF, i.e. sky-view factor (Hesse, 2014; Kokalj *et al.*, 2013).

This last algorithm is the measure of the portion of visible sky and simulates a diffuse illumination over each pixel of the DTM; ultimately, it provides a dimensionless parameter between zero (no visibility) and one (entire hemisphere visible). Comparative analysis proved it particularly suitable when dealing with small topographic depressions (Zakšek *et al.*, 2011; Kokalj *et al.*, 2011).

LiDAR data for our study were acquired between October 2006 and February 2008 with a grid of 1 m × 1 m cells, during a mapping campaign that covered the whole Province of Trento (Figure 3a). All global positioning system (GPS) data are based on the UTM-WGS84 coordinate system. The DTM was freely available on the local Cartographic Portal of Trentino (2006–2008) with a Creative Commons license.

SVF was calculated using SagaGIS (Böhner *et al.*, 2006; Böhner and Antonic, 2009). Considering the relatively small dimension of the target features (see later), we decided to set a low maximum search radius with a value of 10 m (i.e. 10 pixels). Conforming to that suggested by Zakšek *et al.* (2011), we therefore chose a parameter of eight for the number of search directions (Figure 3b).

Object-based shell craters classification and mapping methodology

GeOBIA principles

Hay and Castilla (2008) defined GeOBIA as: 'a sub-discipline of Geographic Information Science (GIScience) devoted to developing automated methods to partition remote sensing imagery into

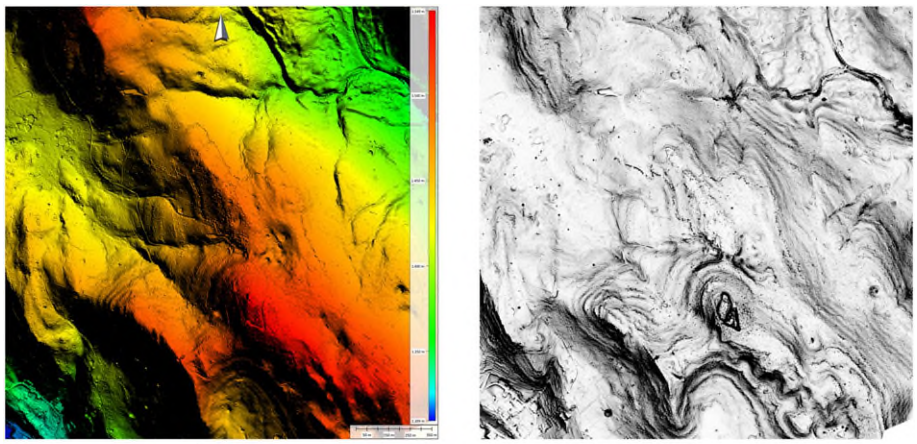

Figure 3. (a) DEM with spatial resolution of 1 m of the study area; (b) SVF visualization of the study area computed in eight directions with a search radius of 10 m. [Colour figure can be viewed at wileyonlinelibrary.com]

meaningful image-objects, and assessing their characteristics through spatial, spectral and temporal scales, so as to generate new geographic information in GIS-ready format.' p 77.

Image-objects are the conceptual unit of this method. They can be described as self-consistent regions created by aggregating proximal pixels according to their spatial, spectral and textural homogeneity, in contrast with the traditional 'per-pixel' approach (Blaschke *et al.*, 2014). This implies a major shift in the protocol of image analysis, because object-based methods take into account shape, pattern and spatial context, thus providing an improved basis for classification and interpretation. The workflow of a GeOBIA project can be broadly divided into four main stages: (1) processing of the image-data; (2) partitioning of the image into primitive image-objects (segmentation); (3) classification of the image-objects to form meaningful geo-objects; (4) post-classification analysis and interpretation.

For a systematic overview of the research on the topic the reader is referred to the comprehensive synthesis of Blaschke (2010).

Features description and parameter evaluation

Paraphrasing the definition of Passmore *et al.* (2014), Millegrobbe and Fort Lusern can be described as 'landscapes of shelling'. In fact, depressions derived from artillery and mortar explosions are one of the characterizing morphologies of the area. The location, number and dimensions of shell holes are key elements to define the extension of the World War I battlefield in the area and to monitor the preservation of the local warscape.

However, despite their peculiar features, artillery craters can easily be misinterpreted on remotely-sensed imagery because of their similarity to other circular depressions typical of mountain environments, such as deforestation holes (*trous avec monticules*), mountain pools, remains of abandoned charcoal pits, ice-storage pits, dolines and sinkholes (De Guio *et al.*, 2013).

In our attempt to identify a method of automatic/discriminant classification, we needed to select a number of parameters that could be used to specifically describe war-related depressions. In this regard, we considered the results of a series of ground surveys focussed on more than a hundred shell holes of World War I on the Grappa massif (Venetian Prealps, Italy). Maximum diameter, maximum depth (approximately 0.5 to 2 m) and difference in level between two extremities were measured and compared (Celi, 1991). The following classification was proposed on the basis of the maximum diameter: (1) less than 2 m; (2) from 2 to 5 m; (3) more than 5 and up to 10 m (with rare exceptions of 15 m).

Hupy and Schaetzl (2006, 2008) report similar results in their study on bombturbation, a form of soil disturbance derived from explosive munitions. In particular, they register a correlation between projectiles calibre and size of the relative depressions, stating that 70 mm shells produced craters of less than 1 m in diameter, while ammunitions with calibre of 420 mm could create depressions larger than 10 m, and several metres deep. World War I craters and further circular depressions can be broadly discriminated according to these values.

All other similar entities are generally characterized by different size, depth or section (Figure 4): mountain pools have a flat bottom and a diameter varying between 7 and 60 m, but usually ranging from 10 to 30 m. Remains of charcoal piles are also flat but only 20–30 cm deep, while ice-storage pits can reach 2 m or even 3 m in depth.

Deforestation holes are similar to shell craters in size, but they present a soil discharge (which is usually located downhill) created during the uprooting of the stumps. Conversely, shell craters have a perimetric ridge produced by the displacement of ground material during the explosion, but in this case the rim is relatively concentric and uniform in width.

Dolines and sinkholes, however, are very difficult to recognize from war-related depressions. It was stated that more than 50% of the artillery craters located in karst environments have been actively evolving into dolines during the last century post-war scenario (Celi, 1991; Sauro, 1993).

Segmentation

Segmentation is the basic step of OBIA. This process aims to divide the image in homogeneous groups of pixels, called image-objects (Haralik and Shapiro, 1985; Hay *et al.*, 1997). Every image-object can be described with a huge set of information attributes (from here on: features) which define its spectral properties, shape, size, texture, context and relations. Primitive image-objects usually do not correspond to geo-objects or real world entities.

For this project, we chose the multiresolution algorithm included in eCognition Developer 9.1 (Trimble Navigation Ltd, Sunnyvale, CA). Multiresolution segmentation is a region growing method: it starts from a single pixel, which is progressively combined to proximal ones according to criteria of minimized intra-object heterogeneity (Baatz and Shäpe, 2000; Benz *et al.*, 2004). We found the selection of the segmentation parameters on a trial and error process based on a group of ground-truth reference depressions, unequivocally identified as shell craters. As a result of these tests, the following values were applied: scale 20, shape 0.1, compactness 0.5 (Figure 5a). The use of a low scale parameter is justified by the small size of the structures to be identified, in order to avoid a possible under-segmentation.

Object-features evaluation and classification training

Geo-objects classification on remotely sensed imagery is a matter of mental models and experience. Literature data discussed earlier were the starting point to identify the most suitable object-features characterizing shell craters.

A classification experiment was first performed in a test section of Millegrobbe (0.6 km × 0.6 km, Figure 6a).

The SVF visualization technique creates a grey scale image, where pure black corresponds to no visibility

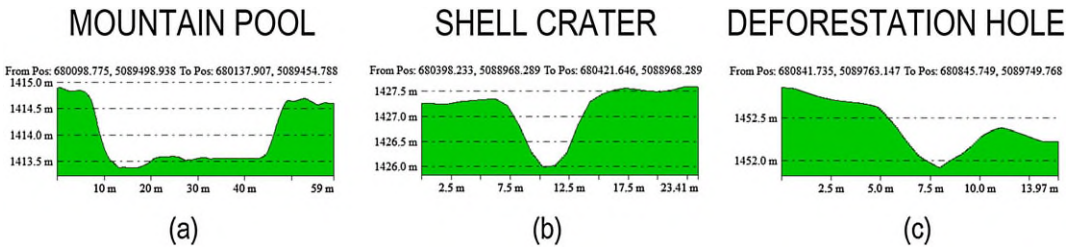

Figure 4. Sections of (a) mountain pool, (b) shell crater, (c) deforestation hole in the study area. [Colour figure can be viewed at wileyonlinelibrary.com]

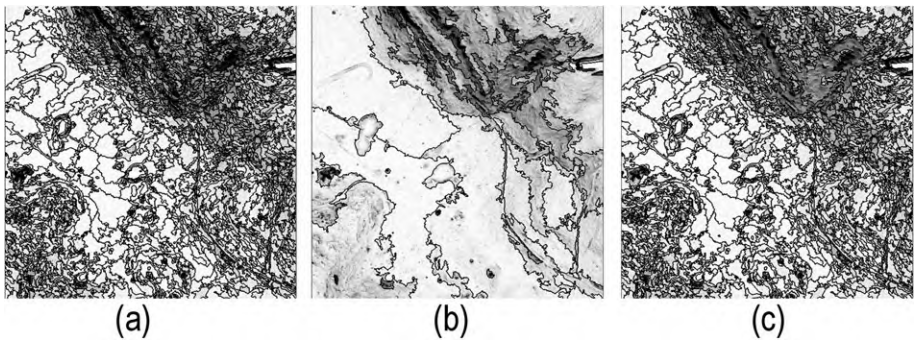

Figure 5. Millegrobbe, multiresolution segmentation with varying scale parameter: (a) 20, (b) 200, (c) 'slope' class: 200 and 'open field' class: 20.

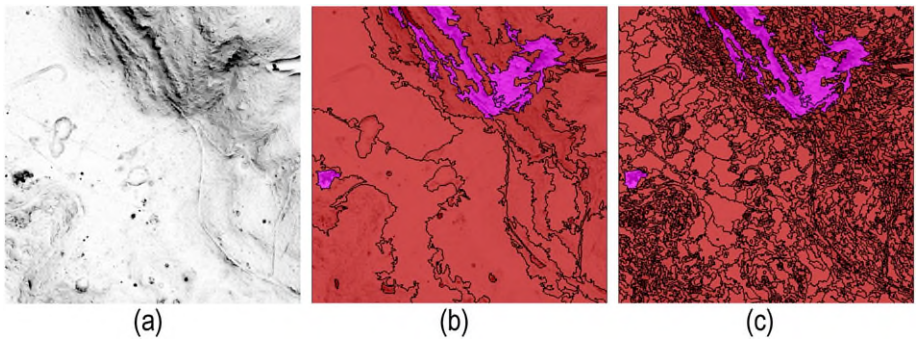

Figure 6. Millegrobbe: (a) detail of the SVF visualization; (b) preliminary landform classification with multiresolution segmentation, scale parameter 200. Red: 'open field' class; pink: 'slope' class; (c) preliminary landform classification with multiresolution segmentation. Red: 'open field' class: scale parameter 20; pink: 'slope' class: scale parameter 200. [Colour figure can be viewed at wileyonlinelibrary.com]

and white to the visibility of the entire hemisphere (Zakšek *et al.*, 2011). In this kind of visualization, shell holes stand out as dark grey/black dots of medium to small size. Sloping areas are also characterized by the presence of similar image-objects due to the recognition of contour lines related to the resolution of our LiDAR data. The dense vegetation canopy in those areas also created a higher concentration of artefacts that could compromise the correct classification. In order to avoid misinterpretations, we first operated a general landform classification of slopes and open fields. For this purpose, we used a higher scale parameter for segmentation (200) and employed the spectral and dimensional properties of the image-objects in order to select those with appropriate mean and area values. In this way, we classified big, dark image-objects as 'slope' and everything else as 'open field' (Figures 5b, 6b).

At this point, we employed a second level segmentation on the class 'open field' with a scale parameter of 20, to optimize the results (Figures 5c, 6c). Subsequently, shape features were applied to identify the 'shell craters' class. Circular shape is one of the more efficient identification parameters for war-related depressions, so we used the object-feature roundness (Figure 7a). Considering the average size of artillery craters in relation to their maximum diameter, as discussed earlier, we opted for the area feature in order to remove larger objects. Despite the wide variability of shell holes radii, we chose a threshold value of 81 m^2 (diameter of approximately 10 m) to avoid a partial overlapping with the mountain pools class (Figure 7b). Additionally, we employed the length/width feature to eliminate the remaining elongated image-objects that were not related with the war-scenario (Figure 7c). Finally, we used the merge region algorithm in order to fuse proximal image-objects and repeated the same object-feature procedure with slightly different parameters (Figure 7d).

At this point 263 on 1699 image-objects were successfully classified as possible shell craters. The parameters used in the project are summarized in Table 1.

Rule-set export

Subsequently, we run the rule-set described earlier on the SVF-based visualization of Cima Campo, Bisele and Millegrobbe, covering an area of approximately 4 km^2 (Figure 8).

The process resulted in 3700 possible artillery craters identified, out of a total of 22 751 image-objects (Figures 9, 10).

The possibility to transfer a classification system from one area to another is problematic, since different sensors, raw data, processing procedures and environmental characteristics may prevent the comparability of the resulting data. However, it is possible to apply the same classification rules to similar areas or to the same area through time, when the raw data and the analytical protocol are consistent: it is a crucial shift in terms of both time saving and landscape monitoring potential. This type of controlled automation is particularly useful when working on large-scale projects because it speeds up the process of features detection and supports the related photo-interpretation.

In our case, the opportunity to apply the same set of rules at a future date will be of central importance to monitor the progressive transformation in size and number of the remaining shell craters and identify strategies to preserve the vanishing World War I heritage.

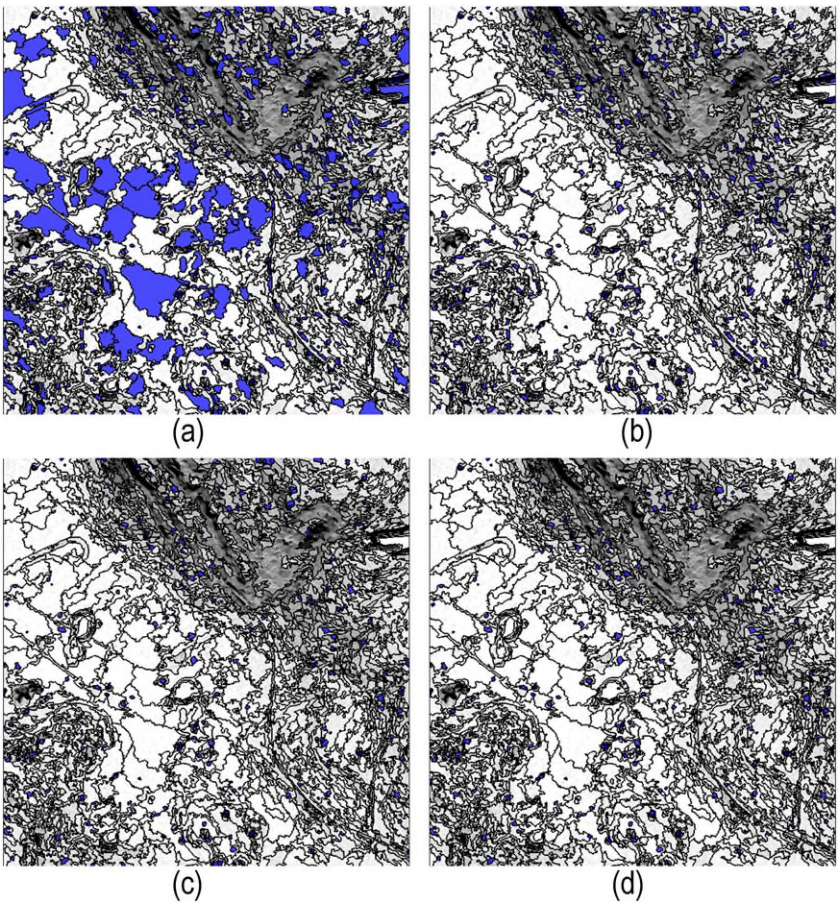

Figure 7. Millegrobbe: shell craters classification-training process. Application of the object features: (a) roundness, (b) area, (c) length-width, (d) final classified image. [Colour figure can be viewed at wileyonlinelibrary.com]

Table 1. Segmentation and object features values of the proposed 'shell craters' rule-set.

—	Object feature	Value	Class
Multiresolution segmentation: scale 200, shape 0.1, compactness 0.5			
1	mean level 1	≤139	SLOPE
2	area level 1	> 620 pixel	
3	unclassified	—	OPEN FIELD
OPEN FIELD multiresolution segmentation: scale 20, shape 0.1, compactness 0.5			
4	OPEN FIELD, roundness	≤1	SHELL CRATERS
5	SHELL CRATERS, area	≥ 81 pixel	unclassified
6	SHELL CRATERS, length/width	> 1.751	unclassified
SHELL CRATERS merge region			
7	SHELL CRATERS, length/width	> 1.751	unclassified
8	SHELL CRATERS, roundness	> 1.093	unclassified
9	SHELL CRATERS, area	≥ 95 pixel	unclassified

Data validation

Field survey

Two sample regions of the analysed area were systematically surveyed to assess the accuracy of the method (Figure 11). The ground control took place in May 2015 and monitored all shell holes within the test-regions. War-related depressions both automatically identified through OBIA and unrecognized by our rule-set were mapped and measured. The fieldwork also allowed for a small number of potential artillery craters to be discounted.

Test area 1 is located in open field and still preserves important traces of World War I trenches and shelling

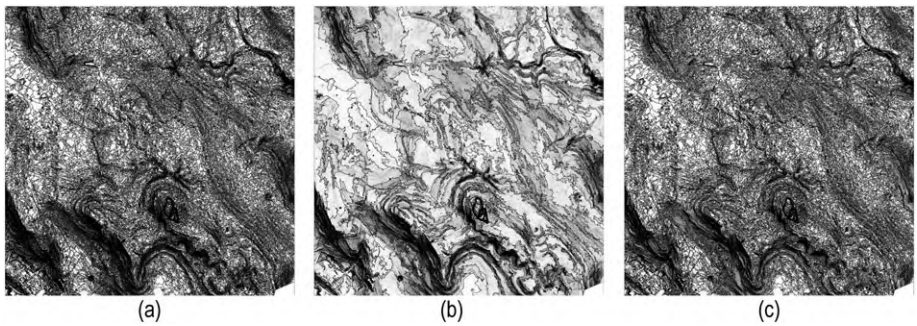

Figure 8. Global test area, multiresolution segmentation with varying scale parameter: (a) 20, (b) 200, (c) 'slope' class: 200 and 'open field' class: 20.

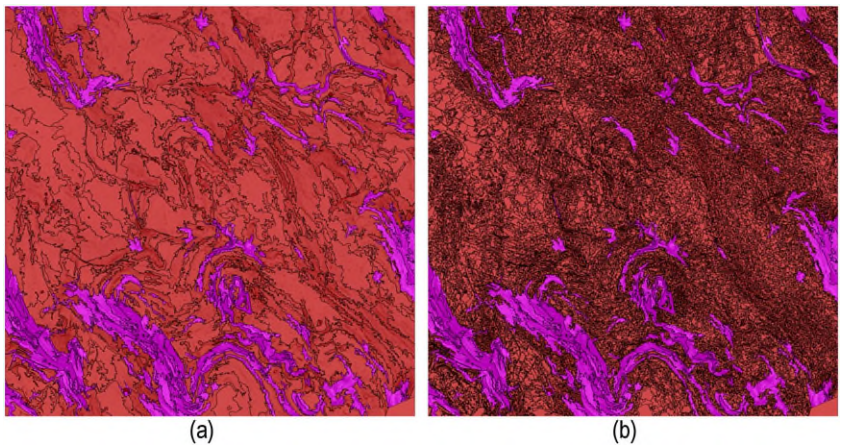

Figure 9. Global test area: (a) preliminary landform classification with multiresolution segmentation, scale parameter 200. Red: 'open field' class; pink: 'slope' class; (b) preliminary landform classification with multiresolution segmentation. Red: 'open field' class: scale parameter 20; pink: 'slope' class: scale parameter 200. [Colour figure can be viewed at wileyonlinelibrary.com]

impact. Seventy-nine possible shell craters identified with the proposed procedure were ground controlled: 70 of them were actually confirmed, while nine were attributed to sub-circular, residual portions of a trench. The survey also identified five additional shell craters: out of these, however, only three exceed 2 m in diameter and had an appreciable depth in the original LiDAR data, so as to be viewed in SVF images.

Test area 2 is located between open fields and forested slopes and preserves no other traces of World War I, except for shell craters. Nevertheless, mountain pools and deforestation holes are frequently found. One hundred and twenty possible war craters where automatically detected in this region and only 15 were discounted at the end of the ground control. Four new occurrences were also located: one of them was too small to be detected (less than 2 m diameter and very shallow), considering the resolution of our LiDAR data, two have a diameter between 2 and 8 m, while one other is above 8 m in size. The latter was not identified because of the decision tree used in the classification; as already reported, the partial overlapping of artillery craters and mountain pools classes led to the discarding of image-objects bigger than 80 m^2, which statistically fell in the class of mountain pools. In this specific case, the result was a loss of information which, however, was unavoidable because of the characteristics of the local landscape.

Results and discussion

Reliability of the OBIA approach and data accuracy calibration

The reliability of the object-based shell craters classification is encouraging, especially considering the residual nature of the structures and the diffuse presence of equivocal elements that could compromise the correct identification.

Table 2 accounts for the number of commission and omission errors ascertained by the ground surveys. In this regard, it should be noted that a small percentage of the omitted artillery craters were not actually visible

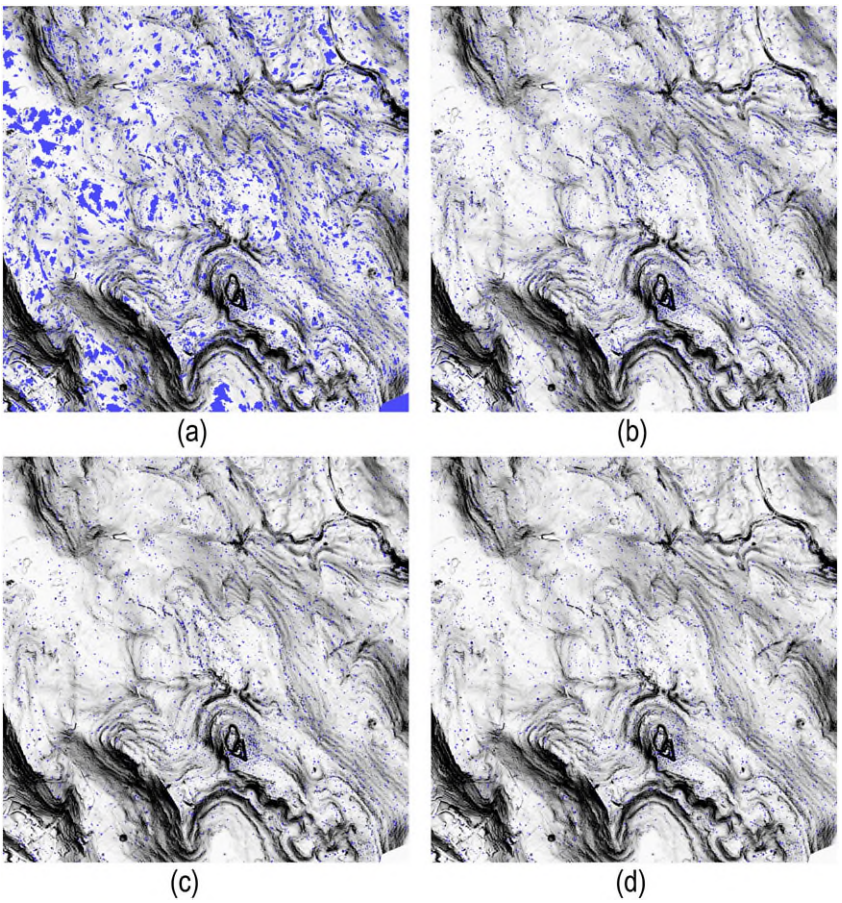

Figure 10. Global test area, with exported rule-set and application of the object features: (a) roundness, (b) area, (c) length-width, (d) final classified image. [Colour figure can be viewed at wileyonlinelibrary.com]

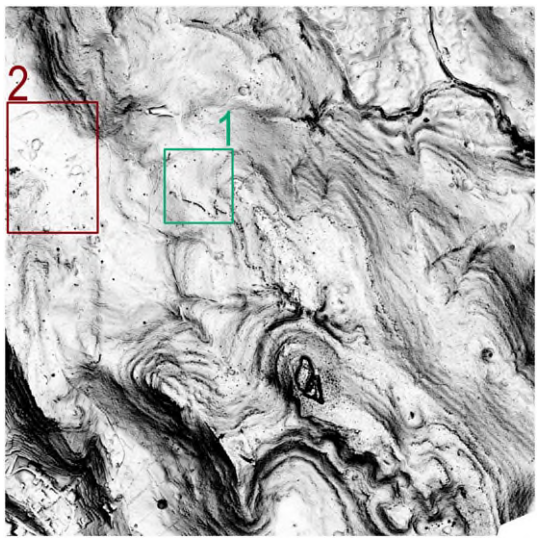

Figure 11. Location of the two survey areas for ground-truth controls on the SVF visualization: test area 1 (green) and test area 2 (red). [Colour figure can be viewed at wileyonlinelibrary.com]

in the SVF, because of LiDAR resolution issues. In addition, the shallowness and the smooth profile of some unidentified craters (depth between 15 and 30 cm, see Figure 12) did not allow SVF to highlight such ground anomalies. Anyway, commission errors were the majority of the inaccuracies encountered. Most of them are related to the presence of artefacts created during the original data collection and processing, which are more frequent in forested slopes. This is why their number is somewhat higher in test area 2.

The values in Table 2 also allow an average standardization of the number of possible shell craters identified in Millegrobbe, Bisele and Fort Lusern with the proposed method. Starting from a non-calibrated amount of 3700 occurrences, we can now hypothesize that approximately 3420 war-related depressions are still present in the area. However, this estimated value considers as single units shell clusters which were fused with the merge region algorithm.

Table 2. Total number of shell craters identified during the ground survey in the two test areas.

—	Test area 1	Test area 2	Total
Image-objects classified as 'shell craters' with the proposed rule-set	79	120	199
Image-objects confirmed as 'shell craters' after the survey	70	105	175
Commission errors	9	15	24
Shell craters omitted by the rule-set classification	5	4	9
Total number of shell craters identified during the survey	75	109	184

Note: Commission and omission errors are also reported in relation to the number of image-objects classified as 'shell craters' by the proposed rule-set.

Figure 12. Examples of the surveyed shell craters: (a) recognized by our rule-set; (b) unrecognized by our rule-set. [Colour figure can be viewed at wileyonlinelibrary.com]

The true positives detected by the described approach can be estimated by multiplying the total number of image-objects classified as shell craters in the entire study area (3700) with the ratio between confirmed image-objects in the test areas (175) and image-objects classified as shell craters in the study areas (199), which returns a value of 3250. This means that 87.8% of the classified image-objects corresponds to real shell craters. Taking into account both commission (approximately 12%) and omission errors (approximately 4%), the average success rate is 84%. The accuracy of the method is thus very high, considering that nowadays the ground traces of the smaller craters are evanescent if not disappeared, but yet it fits very well with what is reported by the historical sources about the area of Cima Campo. In particular, while almost half of the craters created by 280 and 300 mm caliber weapons were probably identified, the smaller ones related to 70 or 150 mm shells got completely lost because of both post-depositional transformations and LiDAR resolution. Craters associated with the explosion of 450 mm artillery and mortars were also omitted to some extent when dealing with areas higher than 80 m^2, in order to avoid the classification of mountain pools.

Conclusions

Despite the problems discussed, this method is a fast, reliable tool to detect, recognize and map shell craters in mountainous areas. The proposed rule-set is an exportable tool that can be used in other landscapes of artillery shelling and aerial bombing, provided that a fine-tune calibration is performed on segmentation and object-features values.

The use of automated or semi-automated feature detection is a theme of central importance in the future developments of archaeological remote sensing. The increasing necessity of objective and reproducible approaches to deal with large amounts of high resolution data and to explore landscape transformations through time imposes a paradigmatic shift in traditional processing methods. As previously noted by Bennett *et al.* (2014), this does not mean that automated classifications can provide historical interpretations. Archaeological operators have indeed a central role in supervised object-oriented analysis, because their knowledge and mental models constitute the basis of the decision tree and the related rule-set.

With this project, the authors strongly encourage the use of a methodology that systematically integrates OBIA and ground truth controls, in order to reach an adequate balance between processing-speed and reliability of the results.

Despite all the examined critical issues, OBIA is a promising innovation in the archaeological field. Our work reveals that a widespread use of this method will be able to improve tremendously the automation rate, the speed, the objectivity and the quality of feature recognition, with no impact at ground level. In particular, this will help in the process of object,

pattern and scenery extraction and classification, providing an economically sustainable tool to catalogue, preserve and protect archaeological heritage.

Acknowledgments

This work was developed as part of L. Magnini's doctoral project funded by a grant of the Provincia Autonoma di Bolzano. The paper was equally prepared by L. Magnini and C. Bettineschi with the supervision of A. De Guio. All authors participated to data interpretation and discussion.

The authors would also like to thank the three anonymous referees for their useful comments and suggestions.

References

Addis A, Angelini I, Nimis P, Artioli G. 2016. Late Bronze Age copper smelting slags from Luserna (Trentino, Italy): Interpretation of the metallurgical process. *Archaeometry* **58**(1): 96–114. DOI:10.1111/arcm.12160.

Artioli G, Angelini I, Nimis P, Villa IM. 2016. A lead-isotope database of copper ores from the southeastern alps: A tool for the investigation of prehistoric copper metallurgy. *Journal of Archaeological Science* **75**: 27–39. DOI:10.1016/j.jas.2016.09.005.

Baatz M, Shäpe A. 2000. Multiresulution segmentation – an optimization approach for high quality multi-scale image segmentation. In Angewandte Geographishe Informationsverarbeitung, volume XII, Strobl J, Blaschke T, Griesebner G (eds). Wichmann: Heidelberg; 12–23.

Balista C, Bagolan M, Cafiero F, *et al.* 1998. Bronze-Age 'Fossil Landscapes' in the Po Plain. In Mensch und Umwelt in der Bronzezeit Europas, Hänsel (ed). Mensch und Umwelt in der Bronzezeit Europas: Kiel; 493–499.

Baratter L. 2007. Dagli Altipiani a Caporetto - Von Hochebene nach Karfreit. Centro di Documentazione: Luserna.

Bennett R, Cowley D, De Laet V. 2014. The data explosion: Tackling the taboo of automatic feature recognition in airborne survey data. *Antiquity* **88**: 896–905.

Benz UC, Hofmann P, Willhauck G, Lingenfelder I, Heynen M. 2004. Multi-resolution, object-oriented fuzzy analysis of remote sensing data for GIS-ready information. *ISPRS Journal of Photogrammetry and Remote Sensing* **58**: 239–258.

Blaschke T. 2010. Object based image analysis for remote sensing. *ISPRS Journal of Photogrammetry and Remote Sensing* **65**: 2–16.

Blaschke T, Hay GJ, Kelly M, *et al.* 2014. Geographic object-based image analysis – towards a new paradigm. *Journal of Photogrammetry and Remote Sensing* **87**: 180–191.

Blaschke T, Lang S, Lorup E, Strobl J, Zeil P. 2000. Object-oriented image processing in an integrated GIS/remote sensing environment and perspectives for environmental applications. In Environmental Information for Planning, Politics and the Public, volume 2, Cremers A, Greve K (eds). Metropolis Verlag: Marburg; 555–570.

Böhner J, Antonic O. 2009. Land-surface parameters specific to topo-climatology. *Geomorphometry – Concepts, Software, Applications, Developments in Soil Science* **33**: 195–226.

Böhner J, McCloy KR, Strobl J (Eds). 2006. SAGA - Analysis and Modelling Applications, volume 115. Göttingen: Göttinger Geographische Abhandlungen.

Cartographic Portal of Trentino. 2006–2008. LiDAR database. http://www.territorio.provincia.tn.it/portal/server.pt/community/lidar/847/lidar/23954

Celi M. 1991. The impact of bombs of World War I on limestone slopes of Monte Grappa. *Proceedings of the International Conference on Environmental Changes in Karst Areas: Quaderni del Dipartimento di Geografia* n. 13 – Università di Padova; 279–287.

De Guio A. 2005. Archeologia di frontiera: il progetto 'Ad Metalla'. In Luserna – La storia di un paesaggio alpino, De Guio A, Zammatteo P (eds). S.A.R.G.O.N: Padova; 87–123.

De Guio A, Betto A, Migliavacca M, Magnini L. 2013. Mountain fossil landscapes and the 'archaeology of us': an object/ pattern/ scenery recognition experiment. In Proceedings of the 5th International Congress of Ethnoarchaeology, ISAO, Rome, 13–14 May 2010, Lugli F, Stoppiello AA, Biagetti S (eds). Archaeopress: Oxford; 241–247.

De Guio A, Magnini L, Bettineschi C. 2015. GeOBIA approaches to remote sensing of fossil landscapes: two case studies from Northern Italy. In Across Space and Time: Papers of the 41st Computer Association and Quantitative Methods in Archaeology Conference (Perth, Australia), Traviglia A (ed). Amsterdam University Press: Amsterdam; 45–53.

Desfossés Y, Jaques A, Prilaux G. 2009. Great War archaeology. Rennes: Ouest-France.

Doneus M, Briese C, Fera M, Janner M. 2008. Archaeological prospection of forested areas using full-waveform airborne laser scanning. *Journal of Archaeological Science* **35**: 882–893. DOI:10.1016/j.jas.2007.06.013.

Dorren LK, Maier B, Seijmonsbergen AC. 2003. Improved Landsat-based forest mapping in steep mountainous terrain using object-based classification. *Forest Ecology and Management* **183**: 31–46.

Fraser AH, Brown M. 2007. Mud, blood and missing men: Excavations at Serre, Somme, France. *Journal of Conflict Archaeology* **3**(1): 147–171. DOI:10.1163/157407807X257412.

Freeland T, Heung B, Burley DV, Clark G, Knudby A. 2016. Automated feature extraction for prospection and analysis of monumental earthworks from aerial LiDAR in the Kingdom of Tonga. *Journal of Archaeological Science* **69**: 64–74.

Gaudio D, Betto A, Vanin S, De Guio A, Galassi A, Cattaneo C. 2013. Excavation and study of skeletal remains from a World War I mass grave. *International Journal of Osteoarchaeology* **25**(5): 585–592.

Gheyle W, Saey T, Van Hollebeeke Y, *et al.* 2016. Historical aerial photography and multi-receiver EMI soil sensing, complementing techniques for the study of a

Great War conflict landscape. *Archaeological Prospection* **23**(3): 149–164. DOI:10.1002/arp.1534.
Halliday S. 2013. I walked, I saw, I surveyed, but what did I see? … and what did I survey? In Interpreting Archaeological Topography: Airborne Laser Scanning, 3D Data and Ground Observation, Opitz R, Cowley DC (eds). Oxbow Books: Oxford; 63–75.
Haralick RM, Shapiro LG. 1985. Image segmentation Techniques. *Computer Vision, Graphics and Image Processing* **29**: 100–132.
Hay GJ, Castilla G. 2008. Geographic object based image analysis (GEOBIA): A new name for a new discipline. In Object Based Image Analysis, Blaschke T, Lang S, Hay G (eds). Springer: Heidelberg; 93–112.
Hay GJ, Niemann KO, Goodenough DG. 1997. Spatial thresholds, image-objects and upscaling: A multi-scale evaluation. *Remote Sensing of Environment* **62**(1): 1–19.
Hentzschel R. 2008. Festungskrieg im Hochgebirge: der Kampf um die österreichischen und italienischen Hochgebirgsforts in Südtirol im Ersten Weltkrieg. Bozen: Athesia.
Hesse R. 2010. LiDAR-derived local relief models – a new tool for archaeological prospection. *Archaeological Prospection* **17**(2): 67–72. DOI:10.1002/arp.374.
Hesse R. 2014. Geomorphological traces of conflict in high-resolution elevation models. *Applied Geography* **46**: 11–20.
Heyman O, Gaston GG, Kimerling AJ, Campbell JT. 2003. A persegment approach to improving aspen mapping from high-resolution remote sensing imagery. *Journal of Forestry* **101**(4): 29–33.
Hupy JP, Schaetzl RJ. 2006. Introducing 'Bombturbation' a singular type of soil disturbance and mixing. *Soil Science* **171**(11): 823–836.
Hupy JP, Schaetzl RJ. 2008. Soil development on the WWI battlefield of Verdun, France. *Geoderma* **145**(1): 37–49.
Jankauskas R, Palubeckaitė-Miliauskienė Ž, Stankevičiūtė D, Kuncevičius A. 2011. Im Osten etwas Neues: Anthropological analysis of remains of German soldiers from 1915-1918. *Anthropologischer Anzeiger* **68**: 393–414.
Kaimaris D. 2011. Location of defensive military trenches in central and northern Greece. *Archaeological Prospection* **18**(3): 223–229.
Kokalj Ž, Zakšek K, Oštir K. 2011. Application of sky-view factor for the visualisation of historic landscape features in lidar-derived relief models. *Antiquity* **85**(327): 263–273.
Kokalj Ž, Zakšek K, Oštir K. 2013. Visualizations of Lidar derived relief models. In Interpreting Archaeological Topography – Airborne Laser Scanning, Aerial Photographs and Ground Observation, Opitz R, Cowley CD (eds). Oxbow Books: Oxford; 100–114.
Korf B, Engeler M, Hagmann T. 2010. The geography of warscape. *Third World Quarterly* **31**(3): 385–399.
Le Bailly M, Landolt M, Bouchet F. 2012. First World War German soldier intestinal worms: An original study of a trench latrine in France. *The Journal of Parasitology* **98**(6): 1273–1275.
Le Roy Ladurie E. 1974. L'histoire immobile. *Annales. Économies, Sociétés, Civilisations* **29**(3): 673–692.
Li Z, Zhu Q, Gold C. 2005. Digital terrain modeling: principles and methodology. CRC Press: Boca Raton, FL.
Maier B, Tiede D, Dorren I. 2008. Characterising mountain forest structure using landscape metrics on LiDAR-based canopy surface models. In Object Based Image Analysis, Blaschke T, Lang S, Hay GJ (eds). Springer: Heidelberg; 625–644.
Masters P, Stichelbaut B. 2009. From the air to beneath the soil – revealing and mapping great war trenches at Ploegsteert (Comines-Warneton), Belgium. *Archaeological Prospection* **16**(4): 279–285.
Mlekuž D, Košir U, Črešnar M. 2016. Landscapes of death and suffering: Archaeology of conflict landscapes of the upper Soča Valley, Slovenia. In Conflict Landscapes and Archaeology from Above, Stichelbaut B, Cowley D (eds). Ashgate: Farnham; 127–146.
Novotny JL. 2009. Digging deeper: Recent publications on First World War archaeology. *Journal of Conflict Archaeology* **5**(1): 273–281.
Passmore DG, Harrison S, Capps TD. 2014. Second World War conflict archaeology in the forests of north-west Europe. *Antiquity* **88**(342): 1275–1290.
Pregesbauer M, Trinks I, Neubauer W. 2014. An object oriented approach to automatic classification of archaeological features in magnetic prospection data. *Near Surface Geophysics* **12**(5): 651–656. DOI:10.3997/1873-0604.2014014.
Robertshaw A, Kenyon D. 2008. Digging the Trenches: The Archaeology of the Western Front. Barnsley: Pen & Sword Military.
Saunders N. 2002. Excavating memories: archaeology and the great war, 1914–2001. *Antiquity* **76**: 101–108.
Saunders N. 2003. Trench Art: Materialities and Memories of War. Berg: Oxford.
Saunders N (Ed). 2012. Beyond the Dead Horizon: Studies in Modern Conflict Archaeology. Oxbow Books: Oxford.
Sauro U. 1993. Human impact on the Karst of the Venetian fore-Alps (Italy). *Environmental Geology* **21**: 115–121.
Sevara C, Pregesbauer M. 2014. Archaeological feature classification: An object oriented approach. *South-eastern European Journal of Earth Observation and Geomatics* **3**(2): 139–143.
Sevara C, Pregesbauer M, Doneus M, Verhoeven G, Trinks I. 2016. Pixel versus object — a comparison of strategies for the semi-automated mapping of archaeological features using airborne laser scanning data. *Journal of Archaeological Science: Reports* **5**: 485–498.
Stal CC, Burgeois J, De Maeyer P, *et al.* 2010. Kemmelberg (Belgium) case study: Comparison of DTM analysis methods for the detection of relicts from the First World War. *Proceeding of the 30th EARSeL Symposium 2010: Remote Sensing for Science, Education, and Natural and Cultural Heritage, Paris, France*; 65–72.
Stichelbaut B, Gheyle W, Saey T, *et al.* 2016. The First World War from above and below. Historical aerial photographs and mine craters in the Ypres Salient. *Applied Geography* **66**: 64–72.
Tommasini A. 1923. Ricordi del tribunale di guerra a Trento, 1914–1918. Arti grafiche Tridentum: Trento.
Verhagen P, Drăguţ L. 2012. Object-based landform delineation and classification from DEMs for

archaeological predictive mapping. *Journal of Archaeological Science* **39**: 698–703.
Weher A, Lohr U. 1999. Airborne laser scanning – an introduction and overview. *ISPRS Journal of Photogrammetry and Remote Sensing* **54**(2–3): 68–82.
Yu Q, Gong P, Chinton N, Biging G, Kelly M, Schirokauer D. 2006. Object based detailed vegetation classification with airborne high spatial resolution remote sensing imagery. *Photogrammetric Engineering & Remote Sensing* **72**(7): 799–811.
Zakšek K, Oštir K, Kokalj Ž. 2011. Sky-view factor as a relief visualization technique. *Remote Sensing* **3**: 398–415.
Zhou Q, Zhu A-X. 2013. The recent advancement in digital terrain analysis and modeling. *International Journal of Geographical Information Science* **27**(7): 1269–1271.